bioengineering

MDPI

Article

Corneal Adhesion Possesses the Characteristics of Solid and Membrane

Jiajin Yang [1], Qiaomei Ren [1], Dong Zhao [1], Zhipeng Gao [1,2,*], Xiaona Li [1,*], Rui He [3] and Weiyi Chen [1]

[1] Department of Biomedical Engineering, Taiyuan University of Technology, Taiyuan 030000, China
[2] State Key Laboratory of Traction Power, Southwest Jiaotong University, Chengdu 610000, China
[3] Department of Excimer Laser, Shanxi Medical University, Taiyuan 030000, China
* Correspondence: gaozhipeng@tyut.edu.cn (Z.G.); lixiaona@tyut.edu.cn (X.L.); Tel.: +86-03513176655 (Z.G. & X.L.)

Abstract: Adhesion behavior usually occurs in corneas associated with clinical treatments. Physiologically, an intact natural cornea is inflated by intraocular pressure. Due to the inflation, the physiological cornea has a mechanical property likeness to membrane. This characteristic is ignored by the classical theory used to analyze the adhesion behavior of soft solids, such as the Johnson–Kendall–Roberts (JKR) model. Performing the pull-off test, this work evidenced that the classical JKR solution was suitable for computing the corneal adhesion force corresponding to the submillimeter scale of contact. However, when the cornea was contacted at a millimeter scale, the JKR solutions were clearly smaller than the related experimental data. The reason was correlated with the membranous characteristic of the natural cornea was not considered in the JKR solid model. In this work, the modified JKR model was superimposed by the contribution from the surface tension related to the corneal inflation due to the intraocular pressure. It should be treated as a solid when the cornea is contacted at a submillimeter scale, whereas for the contact at a larger size, the characteristic of the membrane should be considered in analyzing the corneal adhesion. The modified JKR model successfully described the adhesion characteristics of the cornea from solid to membrane.

Keywords: biomechanics; ophthalmology; JKR theory; adhesion behavior

Citation: Yang, J.; Ren, Q.; Zhao, D.; Gao, Z.; Li, X.; He, R.; Chen, W. Corneal Adhesion Possesses the Characteristics of Solid and Membrane. *Bioengineering* **2022**, *9*, 394. https://doi.org/10.3390/bioengineering9080394

Academic Editor: Xiaofei Wang

Received: 15 July 2022
Accepted: 9 August 2022
Published: 16 August 2022

1. Introduction

The cornea, a transparent organ, forms the anterior pole of the eye, and it plays an essential role in visual function [1]. Adhesion behavior by the cornea is often accompanied with ophthalmic clinical treatments such as wearing contact lenses for correcting myopia [2,3]. After refractive surgeries, the stabilization of the postoperative cornea depends on the corneal cap firmly adhering to the residual stromal bed [4]. Especially, in terms of corneal transplantation, adhesion is a prominent issue of concern regarding biocompatibility; poor interfacial adhesion can affect the clinical outcome of the transplantation [5]. Studying the corneal adhesion, therefore, can help us to preferably understand the biomechanics of the cornea associated with the clinical ophthalmology.

Adhesion behavior is usually determined through a pull-off test, that is, a rigid punch indents onto a solid material and then detaches from it [6–10]. To analyze the adhesion behavior of a solid, the work of adhesion γ, a characteristic of the material, must be considered. There are two classical theories (i.e., the Johnson–Kendall–Roberts (JKR) [11] and Derjaguin–Muller–Toporov (DMT) [12] models) used to analyze the adhesion behaviors of the solids. The DMT and JKR models describe two different types of separation. They derive two different mathematic formulas used to calculate the adhesion force, i.e., $1.5\gamma\pi\boldsymbol{R}$ and $2\gamma\pi\boldsymbol{R}$, with $\boldsymbol{R}$ being the derived radius. The DMT model, related to a strength-limited solution, is suitably used to study brittle failure, whereas the JKR model, related to an energy-limited solution, is suited to analyzing ductile failure [6,9,13]. Due to the fact of excellent compliance, many previous studies have evidenced that the JKR model is suitable

for analyzing the adhesion behaviors of soft materials [14–16], including cancer cells [17] and biological soft tissues [18].

Indeed, employing the JKR model, recently Zhu and colleagues studied and compared the adhesion interactions between the cornea and silicone contact lenses of different types [3]. Their work focused on the interfacial adhesion interaction between the two different soft materials and, thus, the obtained adhesion force was coupled together with contributions from the two soft materials. It is difficult to decouple the adhesion force of the cornea itself from the interaction associated with the two soft materials. Without decoupling, this work performed the pull-off test to study corneal adhesion, employing rigid punches which had a stiffness that exceeded the cornea by many orders of magnitude.

2. Materials and Methods

2.1. Material Preparation

One hundred natural porcine eyes were consecutively collected from a local slaughterhouse, and they were immediately transported to the laboratory within two to three hours after slaughter. In the laboratory, according to the different sizes of the spherical rigid punches, the eyes were divided into seven groups (Supplementary Materials I) to study the scale effect of corneal adhesion through the pull-off test.

2.2. Experimental Protocol

The pull-off test, in this study, was performed at room temperature to determine the adhesion behavior of the cornea itself. Each eye specimen was indented by rigid spherical punches (elastic modulus: ≈200 GPa) with different sizes (Figures 1a and S1). Prior to the indentation test, we removed the other tissues attached to the ocular surface including the extraocular muscles and fats with a pair of scissors and a tweezer at room temperature. As shown in Figure 1a, an eye specimen, with its cornea exposed to the air, was attached to a fixed chamber and fully filled with phosphate-buffered saline (PBS) by negative pressure through an injector, which could simultaneously tune the value of the IOP $\boldsymbol{P}$. We measured the adjusted intraocular pressure with a rebound tonometer (FA800vet, Shanghai, China; resolution: ±1.5–2.0 mmHg) and then measured it again after standing for 30 s. If the intraocular pressure value did not change, the intraocular pressure value of this sample could be determined [10].

Prior to the pull-off test, the IOP value was measured through a rebound tonometer with high interobserver reliability. An Instron 5544 tester (Instron, Boston, USA) with a load cell of 5 N was employed to perform the test. The corresponding resolutions of the force and the displacement were 0.001 N and 0.001 mm, respectively. During the test, a spherical rigid punch was employed to indent the corneal tissue to 2 mN and then detached from it by 1.0 mm/min (Figure 1b). The entire experimental course was carefully observed by capturing images using a DP71 (Olympus, Tokyo, Japan) charge-coupled device (CCD).

Previous studies have defined adhesion behavior. As shown in Figure 1b, it begins at the moment the punch unloads to zero force [19–21] and its whole course can be divided into two steps, i.e., the pull-in and the pull-off. The punch detaches from the contacted cornea to the peak value of the separation force and continues separating from the peak force to the zero force again. The peak value of the separation force is defined as the pull-off force, i.e., the adhesion force, $\boldsymbol{F_{ad}}$.

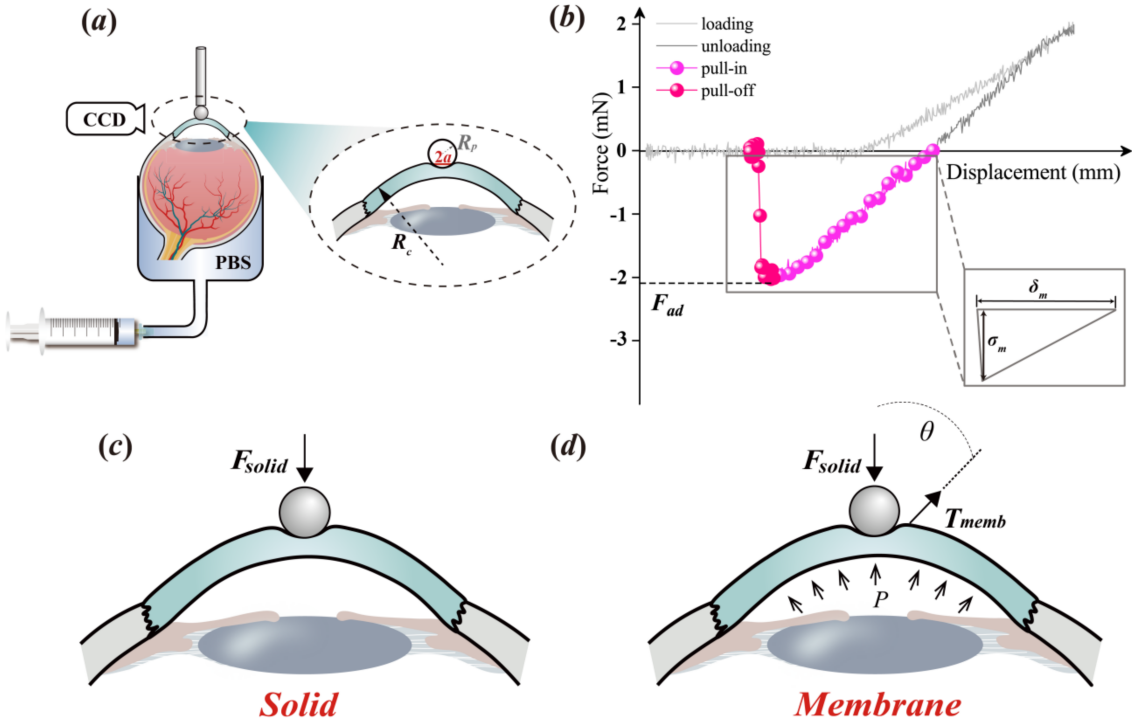

Figure 1. Schematic illustrations for determining corneal adhesion: (**a**) Sketch of the pull-off test in which R_p and R_c, respectively, represent the radii of the punch and the cornea, and a is the related contact radius; (**b**) an example of the experimental data; (**c**,**d**) illustration of the related analytical theory in which F_{solid} represents the adhesion force balanced by the Hertz and the Knedall terms, and T_{memb} represents the surface tension related to the membrane characteristic.

2.3. Theoretical Analysis

Hertz (1896) first solved the contact problem between two rigid spheres [22]. On the basis of the Hertz contact pressure and indentation theory, derived by Sneddon (1965) [23], Johnson et al. (1971) [6] reported the solution of the contact between a rigid sphere and a compliance solid (Figures S2–S4), i.e., the JKR model (derivations in the Supplementary Materials II and III). The related magnitude of the adhesion force solved by the JKR model was $1.5\gamma\pi R$, with $1/R = 1/R_c + 1/R_p$; in this study, R_c and R_p were the radii of the cornea and the punch, respectively (Figure 1a).

Physiologically, the surrounding of a natural cornea is inflated by the IOP. The cornea, therefore, cannot be considered as an absolute solid (Figure 1c); however, it should be suitably considered to superimpose the contributions of the characteristics of a membrane (Figures 1d and S6). This means when analyzing corneal adhesion, the contribution from the surface tension cannot be ignored. Accordingly, in this study, we modified the JKR model through the superposition of the terms of the surface tension [24], which was formulated as follows:

$$F = \frac{4E^*a^3}{3R} - \sqrt{8\pi\gamma E^*a^3} - \alpha P\pi a^2\frac{R_c}{R} \quad (1)$$

where a denotes the contact radius between the spherical rigid punch and the soft cornea; P is the intraocular pressure; and $E^* \approx E_c/(1-\upsilon_c{}^2)$ is the effective elastic modulus, with E_c and υ_c being the elastic modulus and Poisson's ratio of cornea, respectively. It was assumed that the cornea was incompressible and, thus, υ_c was equal to 0.5. Additionally, α is a constant coefficient used to describe the degree of the cornea trending to a membrane. The detailed derivation procedure is shown in the Supplementary Materials V.

To obtain the corneal adhesion force, F_{ad}, in mathematics, one needs to solve the peak value from Equation (1). The definition of F_{ad} is quoted from previous works [25,26], which was used to describe the maximum interfacial force (i.e., pull-off force in the Supplementary

Materials II and III), while the punch is detached from the soft material. To determine the F_{ad} value, in mathematics, one must find the critical contact radius, a_c, in the partial differential solution of $\partial F/\partial a = 0$. Then, a_c *is* substituted into Equation (1), and the calculations result in the obtained F_{ad} value.

In terms of Equation (1), while α *is* equal to zero, this describes the classical JKR solution, consisting of two terms, that is, the Hertz's contact pressure [22] and the Kendall's interfacial adhesion force [27]. In this case, solving the differential equation of $\partial F/\partial a = 0$, one can obtain the value of a_c equal to $(9/8)^{1/3}\left(\gamma\pi R^2/E^*\right)^{1/3}$. Employing a_c into Equation (1), with $\alpha = 0$, one can solve the F_{ad} value as $1.5\gamma\pi R$. On the other hand, while α is equal to one, Equation (1) describes the adhesion behavior of a pure membrane material. With the modified JKR model, $0 < \alpha < 1$, it is hard to obtain analytic solutions. In this study, we obtained the related numerical solutions through the software PyCharm v.3.3 (JetBrains, Prague, Czech).

To solve the magnitudes of the corneal adhesion, two intrinsic characteristics of the cornea, γ and E^*, should be determined. According to previous studies [8,9], if a compliance material exhibits linear adhesion behavior, as shown in the inset of Figure 1b, γ can be simply formulated as $\gamma = \sigma_m\delta_m/2$, where σ_m and δ_m are the maximum adhesion stress and distance, respectively. In terms of E^*, it can be solved through the JKR solution with zero loads, i.e., the Equation (S12) in the Supplementary Materials III, which is formulated as Equation (2):

$$a_0^3 = \frac{3R}{4E^*}(6\gamma\pi R) \tag{2}$$

where a_0 is the contact radius between the punch and the cornea at the moment the experimental data transform from the unloading phase into the pull-in phase (Figure 1b).

2.4. Data Analysis

The related data are presented as the mean ± standard deviation (SD), and they were statistically analyzed through one-way analysis of variance (ANOVA) subjected to an LSD test with the help of SPSS v.24.0 (SPSS Inc., Chicago, IL, USA). A probability value (p) less than 0.05 was considered statistically different.

3. Results

3.1. Corneal Adhesion Was Not Affected by IOP

The experimental results indicated that the corneal adhesion force, F_{ad}, did not vary with the IOPs. As shown in Figure 2a, there were no statistical differences in the F_{ad} values ($p > 0.05$) obtained by the pull-off test during the cornea under the different IOPs in vitro, except for the comparison between the groups of 40 and 60 mmHg obtained through the 1 mm R_p punch.

Interestingly, the related calculations of the two parameters, γ and E^*, were similar to F_{ad}. As shown in Figure 2b,c, regarding punches with a certain radius, the values of γ and E^* also did not vary with the IOPs. There were no statistical differences among the different IOP groups ($p > 0.05$). This phenomenon indicates that the parameters of γ and E^*, obtained here, possessed the intrinsic characteristics of the cornea.

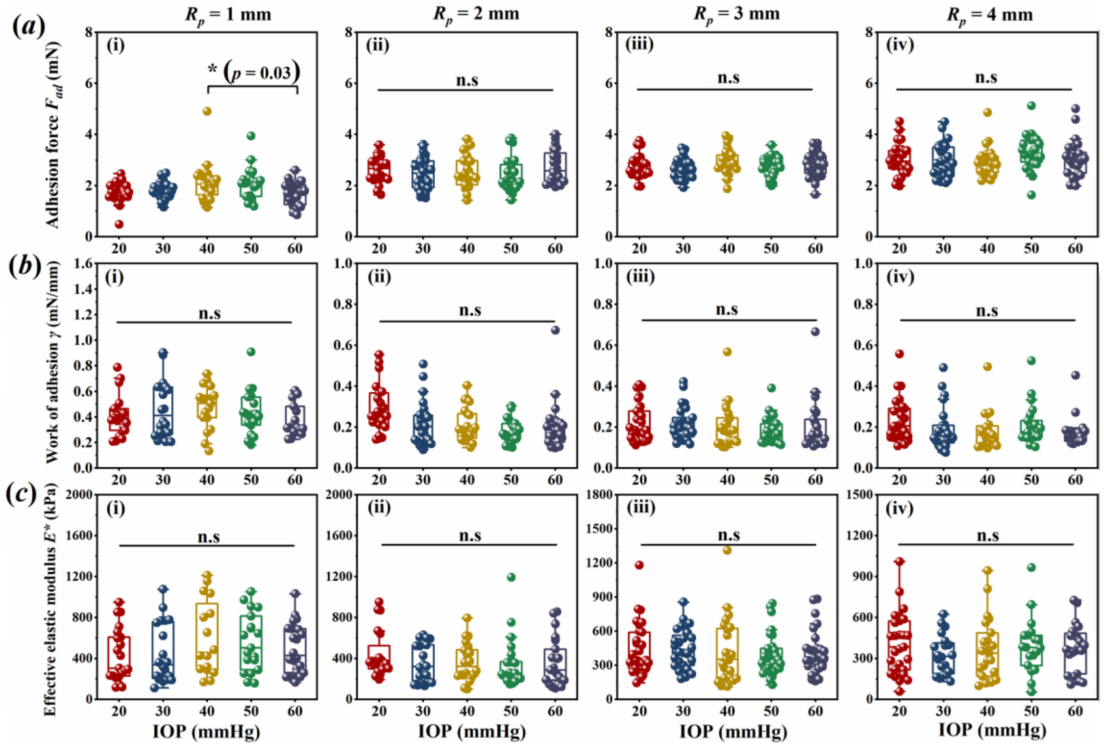

Figure 2. Parameters obtained from the experiment: (**a**) adhesion force (F_{ad}); (**b**) work of adhesion γ; (**c**) effective elastic modulus E^*. (**n.s** indicates no statistical differences among the different groups, with $p > 0.05$ and * $p < 0.05$).

3.2. Scale Effect of Corneal Adhesion

To analyze the scale effect of corneal adhesion, in this study, 20 and 30 mmHg were selected as the internal environment of cornea tolerated, because the normal IOP ranged approximately from 10 to 30 mmHg [28]. Under a normal IOP of 20 or 30 mmHg, as shown in Figure 3, scale effects obviously existed in the corneal adhesion. The parameters γ and E^* exhibited a similar tendency with the function of the punch sizes (Figure 3a,b). For example, under an IOP of 20 mmHg, regarding the punches with submillimeter sizes (i.e., $R_p \leq 1$ mm), both parameters trended towards a decrease with the increase in R_p ($p < 0.05$). When R_p rose to greater than 1 mm, their values trended towards a lack of statistical difference ($p > 0.05$), but they were significantly smaller than those obtained by the punch at the submillimeter scale ($p < 0.01$).

Additionally, the punch sizes could also assuredly affect the F_{ad}. With R_p in the range from 0.5 to 5 mm, used here, the experimental data for F_{ad} trended towards a gradual rise with the increase in R_p (Figure 3c). However, the tendency was very slight when the punch sizes were in the range from 2 to 3 mm ($p > 0.05$). Under an IOP of 20 mmHg, for example, the F_{ad} values obtained through the punches with submillimeter sizes were obviously significantly smaller than those obtained through the larger punch sizes ($p < 0.001$). The minimum value, 1.25 ± 0.25 mN, was obtained by the 0.5 mm R_p punch. It was smaller (1.73 ± 0.39 mN) than that obtained through the 1 mm R_p punch by approximately 28% ($p < 0.01$), and it was twofold smaller than that of the maximum value (3.94 ± 0.73 mN) obtained through the 5 mm R_p punch ($p < 0.001$). The related data are summarized in detail in Table 1.

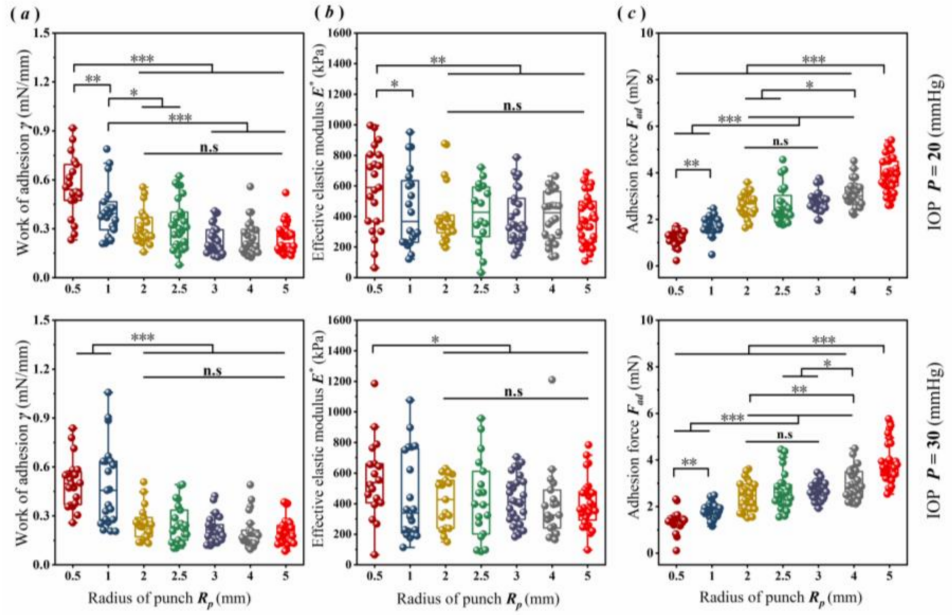

Figure 3. Scale effect of corneal adhesion: (**a**) work of adhesion γ; (**b**) effective elastic modulus E^*; (**c**) adhesion force, F_{ad}, under normal IOPs of 20 and 30 mmHg, respectively (* $p < 0.05$, ** $p < 0.01$, and *** $p < 0.001$; **n.s** indicates no statistical differences among the groups, with $p > 0.05$).

Table 1. The data of γ, E^*, and F_{ad} obtained from the test performed here.

		Radius of Punch R_P (mm)						
	IOP *P* (mmHg)	**0.5**	**1**	**2**	**2.5**	**3**	**4**	**5**
γ (mN/mm)	20	0.56 ± 0.19	0.41 ± 0.16	0.29 ± 0.12	0.33 ± 0.15	0.22 ± 0.09	0.23 ± 0.11	0.24 ± 0.09
	30	0.50 ± 0.15	0.46 ± 0.22	0.22 ± 0.11	0.27 ± 0.15	0.22 ± 0.08	0.19 ± 0.11	0.21 ± 0.08
	40		0.47 ± 0.17	0.21 ± 0.08		0.20 ± 0.10	0.18 ±0.09	
	50		0.43 ± 0.17	0.18 ± 0.06		0.18 ± 0.06	0.21 ± 0.10	
	60		0.37 ± 0.13	0.21 ± 0.12		0.20 ± 0.13	0.18 ± 0.08	
E^* (kPa)	20	581.52 ± 275.10	434.18 ± 260.89	437.73 ± 231.14	777.24 ± 500.72	434.92 ± 235.09	407.72 ± 224.77	381.59 ± 161.94
	30	560.80 ± 255.80	449.18 ± 292.02	361.16 ± 184.86	713.89 ± 382.38	441.29 ± 174.80	328.57 ± 145.96	403.92 ± 160.92
	40		601.36 ± 365.53	360.25 ± 182.63		422.27 ± 285.37	363.36 ± 224.58	
	50		558.01 ± 282.76	357.27 ± 247.15		393.64 ± 185.03	395.25 ± 205.55	
	60		492.78 ± 243.71	366.89 ± 237.06		418.69 ± 200.53	377.33 ± 177.10	
F_{ad} (mN)	20	1.25 ± 0.25	1.73 ± 0.39	2.62 ± 0.50	2.62 ± 0.79	2.76 ± 0.46	3.00 ± 0.61	3.94 ± 0.73
	30	1.37 ± 0.43	1.81 ± 0.32	2.47 ± 0.62	2.62 ± 0.79	2.66 ± 0.39	3.00 ± 0.64	3.88 ± 0.87
	40		2.10 ± 0.73	2.56 ± 0.64		2.94 ± 0.47	2.94 ± 0.58	
	50		2.07 ± 0.59	2.42 ± 0.66		2.75 ± 0.38	3.29 ± 0.68	
	60		1.69 ± 0.45	2.74 ± 0.64		2.84 ± 0.49	3.05 ± 0.70	

3.3. Analysis Employing the JKR Models

Substituting the obtained values of γ and E^* into the classical and modified JKR models, we calculated the F_{ad} values and compared them with the experimental data. The comparisons showed that the classical JKR model should not be used to adequately describe corneal adhesion, except for contact that has occurred at the submillimeter scale.

The experimental data for F_{ad}, as shown in Figure 4a, were well fitted using the classical JKR solutions when the cornea contacted with the 1 mm R_p punch. However, for the punches with larger sizes (Figure 4b–d), such as the 3 mm R_p, the F_{ad} values calculated by the JKR model were much smaller than the experimental data when the corneas had higher IOPs than normal levels (Figure 4c). Under an IOP of 40 mmHg, for example, the F_{ad} value calculated using the JKR model (1.90 ± 0.76 mN) was smaller than the experimental data (2.94 ± 0.47 mN) by approximately 35% (Figure 4c). These errors were compensated for using the modified JKR solutions (Figure 4b–d).

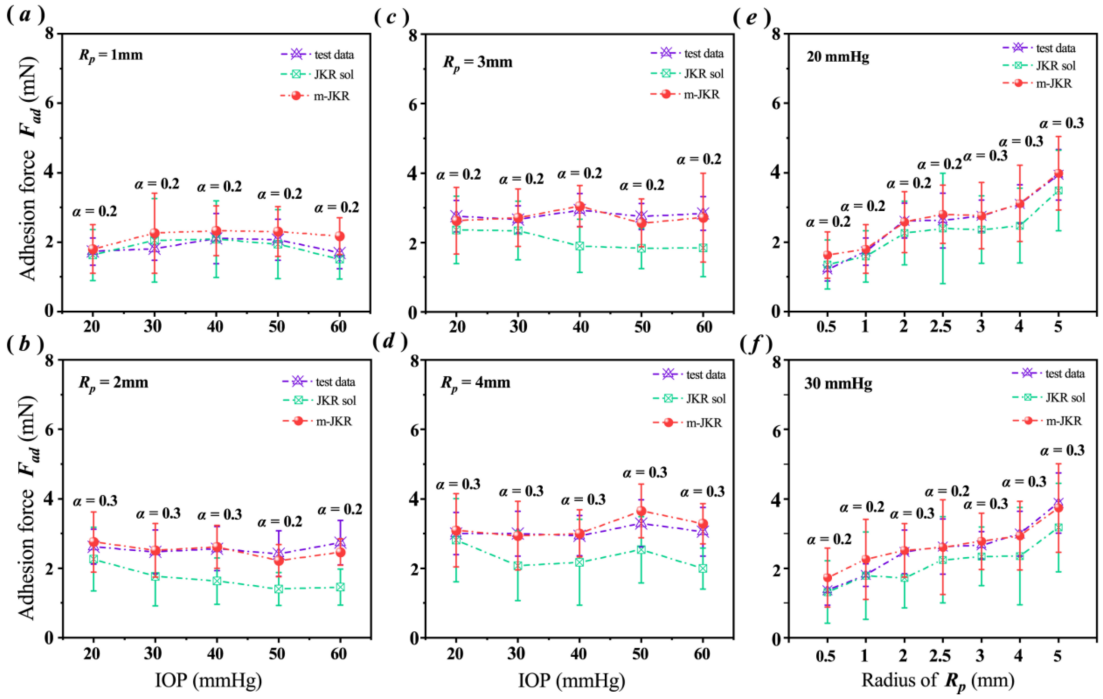

Figure 4. Comparisons of the corneal adhesion force, F_{ad}, obtained from the experiment and theories: (**a**–**d**) show comparisons of the different IOPs; (**e**,**f**) show comparisons of the scale effect of the corneal adhesion under the normal IOPs of 20 and 30 mmHg. The data are presented as the mean ± SD; JKR sol and m-JKR indicate the solutions from the JKR and modified JKR models, respectively.

The related scale variations described and shown in Figures 4e,f and S5 could evidence the tendency of corneal adhesion. Compared with the experimental data, both the classical and the modified JKR solutions obtained similar tendencies as functions of F_{ad} and R_p. Unlike the modified JKR solutions, however, the related trend obtained by the JKR solutions was lower than the experimental data. Except for the submillimeter R_p, the JKR solutions were obviously smaller than the one-to-one correspondence experimental F_{ad} values. On the contrary, in terms of the R_p in the millimeter scales, the trend displayed by the modified JKR solutions was well matched with the experimental data (Figures S2 and 4e,f).

4. Discussion

This work reports that the corneal adhesion possessed a scale effect, affected by the contact area. In this study, the classical JKR model, used to describe the adhesion of solids, was valid for the analysis of corneal adhesion at submillimeter sizes (Figure 4a). However, its validity decreased with the increase in the contact area. When the punch sizes were at the millimeter scale, the corneal F_{ad} obtained by the JKR solutions were obviously smaller than the related experimental data (Figure 4b–f).

This contradiction was observed between the JKR solutions and the experimental data, implying that the JKR model partially failed to analyze the corneal adhesion. To understand the reason for this, we deemed that the emphasis should be on the physiology of the natural cornea, which is fully inflated by IOP, like a membrane. To analyze corneal adhesion, therefore, the contribution of the membranous characteristic should be considered. This important factor, however, is not considered in the classical JKR model.

According to the results of the comparison, it was clear that the scale effect of corneal adhesion is associated with the variation of its characteristics from a solid to membrane. In the case that the punch size is sufficiently smaller (i.e., submillimeter scale) than the cornea, the cornea should be considered as a solid, and the classical JKR model could obtain the suitable solution (Figure 4a). Whereas when the punch size was within the millimeter scale, the cornea increasingly trended towards the characteristic of a membrane. Thus,

a suitable solution for corneal adhesion should be obtained by the modified JKR model proposed here.

To simply describe the scale effect of corneal adhesion, a dimensionless normalization analysis was employed here. The factors related to corneal adhesion contained adhesion force, work of adhesion, elastic modulus, geometry, IOPs, etc. With these factors taken into account, this work proposed a parameter, κ, formulated as Equation (3), to describe the scale effect.

$$\kappa = \left(\frac{F_{ad}\gamma}{PE^{*}a_c^3} \right)^{\frac{1}{3}} \quad (3)$$

The parameter κ, in this study, was described as a function of the ratio between the radii of the punch and the cornea: R_p/R_c. The average value of the corneal radius used here was 9.58 ± 0.22 mm. Compared with the tendencies described in Figure 4e,f, interestingly, the normalization tendencies, as a function of κ and R_p/R_c, exhibited the opposite (Figure 5). As shown in Figure 5, the κ values decreased with the increase in the ratio R_p/R_c, and the related data were well fitted by an exponential function. For example, in terms of the cornea under the normal IOP of 20 mmHg (Figure 5a), while the punch was infinitesimal (i.e., the ratio of R_p/R_c boundlessly approaches to zero), the κ value was increasingly closer to 1.05, and the corneal adhesion increasingly trended toward the characteristic of a solid. Inversely, while the punch size was infinitely great, it was similar to an intact cornea contacted to the ground; the κ value was increasingly closer to approximately 0.29, and the corneal adhesion increasingly trended toward the characteristic of a membrane (Figure 5a). Although the normalization tendencies reversed to the dimensional, the related discrepancies between the experimental and theoretical data were the same. Compared with the experimental data, the classical JKR solutions also obtained a lower normalization tendency, and this error could also be offset by the modified JKR solutions (insets in Figure 5).

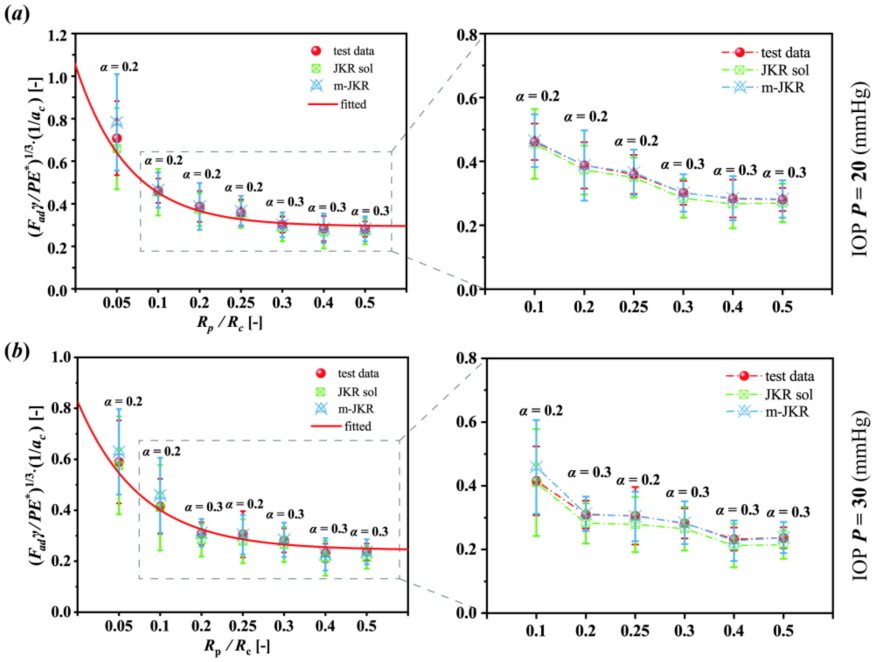

Figure 5. Normalization analysis of the scale effect of corneal adhesion: (**a**) under 20 mmHg, the fitting exponential function was $y = 0.76\ exp\ (-12.53x) + 0.29$; (**b**) under 30 mmHg, the fitting exponential function was $y = 0.58\ exp\ (-10.49x) + 0.24$. The data are presented as the mean ± SD; JKR sol and m-JKR indicate the solutions from the JKR and modified JKR models, respectively.

Consequently, this work evidenced that corneal adhesion possessed a scale effect due to the fact of its characteristics varying from a solid to a membrane. When a cornea was contacted by a smaller punch, within the submillimeter range, its adhesion could be

described by the theory related to solids, i.e., the JKR model. While with greater contact areas, however, to analyze the corneal adhesion, the contribution of the surface tension needed considering. With an increasing contact area, the corneal adhesion increasingly trended toward a membrane. The related evidence was revealed in the results of the comparison, as shown in Figures 4, 5 and S5. Without wet conditions, this study related to corneal adhesion also supported the previous discovery that the scale effect existed in the wet adhesion of biological attachment systems [29].

Clinically, corneal adhesion usually appears with a greater contact area at the millimeter scale. In terms of refractive surgeries, for example, the optical operation diameters were in the range of 5–8 mm [30,31]. Wearing commercial contact lenses and corneal transplantation can cover the whole or partial surface of the cornea. Additionally, it is of great significance to study adhesives to repair corneal wounds. The current common closure methods, such as stromal hydration, suture, and wound sealant, have been reported [32]. It is clinically meaningful to study changes in corneal adhesion after using these methods. To understand the adhesion behavior of the cornea itself, this work provided a suitable theory by modifying the classical JKR model.

Compared with similar published works [3,33], this present work found that the F_{ad} values of the cornea were smaller than the previous studies by one or two orders of magnitude. This is because the contact areas observed here, between the cornea and the punch, were much smaller than previous works related to corneas contacted with artificial corneas or contact lenses. The measured F_{ad} value depended on the contact area (Figure 3). The F_{ad} of the natural cornea was approximately 20 mN, related to the adhesion interaction between the Boston keratoprosthesis and corneal disk samples with a radius of 3 mm [33]. However, the maximum critical contact radius obtained here, a_c, related to the 5 mm R_p punch, with a cornea IOP under 20 mmHg, was approximately 0.34 mm (Table S1).

Additionally, rate dependence [34] and a time effect [35] obviously existed in the viscoelastic soft materials during the loading speed under the medium and high strain rates. However, under a quasi-static state, when the indentation speed was less than 500 μm/s, the adhesion characteristic of the tested soft material was stable [36]. In addition, Dai et al. indicated that the adhesion energy of soft matters due to the hydrodynamic force or the viscous force could be negligible when the speed was lower than 0.5 mm/s [25]. In this study, 1 mm/min (i.e., approximately 17 μm/s) was used as the indentation speed. Therefore, in this study, the viscous effects on the adhesion behavior determined here could also be negligible.

In summary, this study evidenced that corneal adhesion possessed a scale effect. It should be treated as a solid when the cornea is contacted at the submillimeter scale, whereas for contact of a larger size, the characteristic of a membrane should be considered when analyzing the corneal adhesion. The modified JKR model proposed here successfully described the adhesion characteristics of the cornea from a solid to membrane.

5. Conclusions

This study evidenced that corneal adhesion possessed a scale effect. It should be treated as a solid when the cornea is contacted at the submillimeter scale, whereas when the contact is of a larger size, the characteristic of a membrane should be considered when analyzing the corneal adhesion. The modified JKR model was superimposed by the contribution from the surface tension related to the characteristic of membrane. Where the coefficient α used to describe the degree of the cornea trending to membrane, while α equals zero, it describes the classical JKR solution. The modified JKR model proposed here successfully described the adhesion characteristics of the cornea from a solid to membrane.

Supplementary Materials: The following supporting information can be downloaded at: https://www.mdpi.com/article/10.3390/bioengineering9080394/s1, Figure S1: Images captured through CCD; Figure S2: Sketching for a flat-cylindrical punch indents a semi-infinite solid; Figure S3: Sketching for a rigid punch detaches from a soft material; Figure S4: Sketching for the contaction mechanics between two spheres; Figure S5: Supplementary comparisons of the corneal adhesion

force F_{ad} obtained from the experiment and theories, including the JKR solutions and the modified JKR solutions with α equals to 0.1, 0.2, 0.3, 0.4, and 0.5; Figure S6: The contaction between a small rigid sphere between an inflated thin-spherical film; Table S1: The detailed experimental data of each cornea under normal IOP of 20 mmHg.

Author Contributions: Z.G. designed this work guided by X.L. and W.C., J.Y., D.Z. and Z.G. performed the pull-off test. J.Y., Z.G., Q.R. and R.H., analyzed the experimental data. Q.R. and J.Y. sketched the related illustration graphs. Z.G. derived the related theory, guided by W.C., Z.G., J.Y. and X.L. executed the writing of the manuscript. All authors have read and agreed to the published version of the manuscript.

Funding: This research was funded by the National Natural Science Foundation of China, grant numbers 31800789, 12072218, 11872262, and 12172243.

Institutional Review Board Statement: The animal study protocol was approved by the Ethics Committee of Taiyuan University of Technology (protocol code TYUT202107084 and date of approval is 29 July 2021).

Informed Consent Statement: Not applicable.

Data Availability Statement: All data generated or analyzed during this study are included in this published article (and its Supplementary Information files).

Acknowledgments: Thanks to the National Natural Science Foundation of China for funding this research and to the authors for their contributions.

Conflicts of Interest: The authors declare no conflict of interest.

References

1. Riau, A.K.; Liu, Y.C.; Yam, G.H.; Mehta, J.S. Stromal keratophakia: Corneal inlay implantation. *Prog. Retin. Eye Res.* **2020**, *75*, 100780. [CrossRef]
2. Yu, Y.; Hsu, K.H.; Gharami, S.; Butler, J.E.; Hazra, S.; Chauhan, A. Interfacial polymerization of a thin film on contact lenses for improving lubricity. *J. Colloid Interface Sci.* **2020**, *571*, 356–367. [CrossRef]
3. Zhu, D.; Liu, Y.; Gilbert, J.L. Micromechanical measurement of adhesion of dehydrating silicone hydrogel contact lenses to corneal tissue. *Acta Biomater.* **2021**, *127*, 242–251. [CrossRef]
4. Khamar, P.; Shetty, R.; Vaishnav, R.; Francis, M.; Nuijts, R.M.; Sinha Roy, A. Biomechanics of LASIK flap and SMILE cap: A prospective, clinical study. *J. Refract. Surg.* **2019**, *35*, 324–332. [CrossRef] [PubMed]
5. Sharifi, R.; Mahmoudzadeh, S.; Islam, M.M.; Koza, D.; Dohlman, C.H.; Chodosh, J.; Gonzalez-Andrades, M. Covalent Functionalization of PMMA Surface with L-3, 4-Dihydroxyphenylalanine (L-DOPA) to Enhance its Biocompatibility and Adhesion to Corneal Tissue. *Adv. Mater. Interfaces* **2020**, *7*, 1900767. [CrossRef]
6. Johnson, K.L.; Kendall, K.; Roberts, A.D. Surface energy and the contact of elastic solids. *Proc. Math. Phys. Eng. Sci.* **1971**, *324*, 301–313.
7. Cho, H.; Wu, G.; Christopher Jolly, J.; Fortoul, N.; He, Z.; Gao, Y.; Yang, S. Intrinsically reversible superglues via shape adaptation inspired by snail epiphragm. *Proc. Natl. Acad. Sci. USA* **2019**, *116*, 13774–13779. [CrossRef]
8. Jiang, Y.; Grierson, D.S.; Turner, K.T. Flat punch adhesion: Transition from fracture-based to strength-limited pull-off. *J. Phys. D Appl. Phys.* **2014**, *47*, 325301. [CrossRef]
9. Peng, B.; Feng, X.Q.; Li, Q. Decohesion of a rigid flat punch from an elastic layer of finite thickness. *J. Mech. Phys. Solids* **2020**, *139*, 103937. [CrossRef]
10. Ren, Q.; Chen, J.; Li, X.; Lv, Y.; Niu, X.; Chen, W.; Gao, Z. Effective elastic modulus of an intact cornea related to indentation behavior: A comparison between the Hertz model and Johnson-Kendall-Roberts model. *Exp. Eye Res.* **2021**, *209*, 108670. [CrossRef]
11. Johnson, K.L.; Greenwood, J.A. An adhesion map for the contact of elastic spheres. *J. Colloid Interface Sci.* **1997**, *192*, 326–333. [CrossRef]
12. Derjaguin, B.V.; Muller, V.M.; Toporov, Y.P. Effect of contact deformations on the adhesion of particles. *J. Colloid Interface Sci.* **1975**, *53*, 314–326. [CrossRef]
13. Tang, T.; Hui, C.Y. Decohesion of a rigid punch from an elastic layer: Transition from "flaw sensitive" to "flaw insensitive" regime. *J. Polym. Sci. Pol. Phys.* **2005**, *43*, 3628–3637. [CrossRef]
14. Ciavarella, M.; Joe, J.; Papangelo, A.; Barber, J.R. The role of adhesion in contact mechanics. *J. R. Soc. Interface* **2019**, *16*, 20180738. [CrossRef]
15. Xia, G.; Huang, Y.; Su, Y.; Chen, W. Exact axisymmetric adhesive contact analysis for a pre-deformed soft electroactive half-space. *Int. J. Solids Struct.* **2020**, *207*, 206–229. [CrossRef]

16. Kuhar, K.; Jesbeer, M.; Ghatak, A. Soft Gel-Filled Composite Adhesive for Dry and Wet Adhesion. *ACS Appl. Polym. Mater.* **2021**, *3*, 3755–3765. [CrossRef]
17. Hu, J.; Youssefian, S.; Obayemi, J.; Malatesta, K.; Rahbar, N.; Soboyejo, W. Investigation of adhesive interactions in the specific targeting of Triptorelin-conjugated PEG-coated magnetite nanoparticles to breast cancer cells. *Acta Biomater.* **2018**, *71*, 363–378. [CrossRef]
18. Wu, G.; Gotthardt, M.; Gollasch, M. Assessment of nanoindentation in stiffness measurement of soft biomaterials: Kidney, liver, spleen, and uterus. *Sci. Rep.* **2020**, *10*, 18784. [CrossRef]
19. Lai, Y.; He, D.; Hu, Y. Indentation adhesion of hydrogels over a wide range of length and time scales. *Extreme Mech. Lett.* **2019**, *31*, 100540. [CrossRef]
20. Li, Y.; Huang, S.; Wei, C.; Wu, C.; Mochalin, V.N. Adhesion of two-dimensional titanium carbides (MXenes) and graphene to silicon. *Nat. Commun.* **2019**, *10*, 3014. [CrossRef]
21. Deng, W.; Kesari, H. Effect of machine stiffness on interpreting contact force–indentation depth curves in adhesive elastic contact experiments. *J. Mech. Phys. Solids* **2019**, *131*, 404–423. [CrossRef]
22. Hertz, H. *Miscellaneous Papers*; Macmillan: London, UK, 1896.
23. Sneddon, I.N. The relation between load and penetration in the axisymmetric Boussinesq problem for a punch of arbitrary profile. *Int. J. Eng. Sci.* **1965**, *3*, 47–57. [CrossRef]
24. Fung, Y. *Biomechanics: Mechanical Properties of Living Tissues*; Springer Science & Business Media: Berlin/Heidelberg, Germany, 2013.
25. Dai, A.N.; He, W.; Wang, S.B.; Chen, W.J.; Li, C.W.; Wang, Z.Y.; Li, L.A. In vivo adhesive behavior of human facial skin by a modified indentation test. *J. Mech. Behav. Biomed. Mater.* **2019**, *92*, 172–178. [CrossRef]
26. Morales-Hurtado, M.; de Vries, E.G.; Peppelman, M.; Zeng, X.; Van Erp, P.E.J.; van der Heide, E. On the role of adhesive forces in the tribo-mechanical performance of ex vivo human skin. *Tribol. Int.* **2017**, *107*, 25–32. [CrossRef]
27. Kendall, K. The adhesion and surface energy of elastic solids. *J. Phys. D Appl. Phys.* **1971**, *4*, 1186. [CrossRef]
28. Yang, W.; Meyers, M.A.; Ritchie, R.O. Structural architectures with toughening mechanisms in Nature: A review of the materials science of Type-I collagenous materials. *Prog. Mater. Sci.* **2019**, *103*, 425–483. [CrossRef]
29. Qian, J.; Gao, H. Scaling effects of wet adhesion in biological attachment systems. *Acta Biomater.* **2006**, *2*, 51–58. [CrossRef]
30. Busin, M.; Leon, P.; Nahum, Y.; Scorcia, V. Large (9 mm) deep anterior lamellar keratoplasty with clearance of a 6-mm optical zone optimizes outcomes of keratoconus surgery. *Ophthalmology* **2017**, *124*, 1072–1080. [CrossRef] [PubMed]
31. Zhang, J.H.; Wang, S.R.; He, Y.X.; Yao, B.Y.; Zhang, Y. The best optical zone for small-incision lenticule extraction in high myopic patients. *J. Cataract. Ref. Sur.* **2020**, *46*, 1302–1307. [CrossRef] [PubMed]
32. Zhang, S.; Zhou, H.; Huang, C.; Sun, J.; Qu, X.; Lu, Y. A novel corneal adhesive based on functionally coupled PEG-lysozyme hydrogel for wound closure after surgical eye surgery. *Chin. Chem. Lett.* **2022**, *33*, 4321–4325. [CrossRef]
33. Sharifi, S.; Sharifi, H.; Guild, C.; Islam, M.M.; Tran, K.D.; Patzer, C.; Chodosh, J. Toward electron-beam sterilization of a pre-assembled Boston keratoprosthesis. *Ocul. Surf.* **2021**, *20*, 176–184. [CrossRef]
34. Afferrante, L.; Violano, G. On the effective surface energy in viscoelastic Hertzian contacts. *J. Mech. Phys. Solids* **2022**, *158*, 104669. [CrossRef]
35. Lyashenko, I.A.; Popov, V.L. The effect of contact duration and indentation depth on adhesion strength: Experiment and numerical simulation. *Tech. Phys.* **2020**, *65*, 1695–1707. [CrossRef]
36. Pailler-Mattei, C.; Zahouani, H. Analysis of adhesive behaviour of human skin in vivo by an indentation test. *Tribol. Int.* **2006**, *39*, 12–21. [CrossRef]